P H Y S I C A L   R E V I E W   L E T T E R S

Theory of Laser Acceleration of Light-Ion Beams from Interaction of Ultrahigh-Intensity Lasers with Layered Targets

B. J. Albright, L. Yin, B. M. Hegelich, Kevin J. Bowers,* T. J. T. Kwan, and J. C. Fernández

Los Alamos National Laboratory, Los Alamos, New Mexico 87545, USA
(Received 18 August 2005; published 15 September 2006)

Experiments at the LANL Trident facility demonstrated the production of monoenergetic ion beams from the interaction of an ultraintense laser with a target comprising a heavy ion substrate and thin layer of light ions. An analytic model is obtained that predicts how the mean energy and quality of monoenergetic ion beams and the energy of substrate ions vary with substrate material and light-ion layer composition and thickness. Dimensionless parameters controlling the dynamics are derived and the model is validated with particle-in-cell simulations and experimental data.

The generation of energetic ion beams from ultrahigh intensity lasers is an area of active research. Experiments produce accelerating E fields of over 10 TV/m at the backs of thin (10 s of μm) laser-driven solid targets. These fields, surpassing those in conventional accelerators by 6 orders of magnitude, accelerate ion beams with kA and above currents and transverse emittances below $10^{-3}\pi$ mm mrad. These beam characteristics enable compact, high fluence accelerators suitable for applications such as radiography, nuclear physics, inertial confinement fusion, and medical applications. Protons have been accelerated to >60 MeV [1] and energetic, higher-Z ions have also been produced [2,3].

A hallmark of ion energy spectra in these experiments is their broad range of energies, with a preponderance of low-energy (and relatively few high-energy) ions [1,2,4]. This is inadequate for applications where monoenergetic ions are required [5]. Recent experiments at the LANL Trident facility produced, for the first time, monoenergetic multi-MeV light-ion beams (3 MeV/nucleon C^{5+} ions—FWHM of 0.5 MeV/nucleon) using a sub-ps laser pulse with a 20 μm palladium target that had a thin layer of carbon (<1 monolayer) on the back surface of the target [6]. (Similar spectra were reported in proton acceleration experiments [7]). During acceleration, carbon ions detach from the substrate and accelerate in the hot electron sheath at the back of the foil, consistent with particle-in-cell (PIC) [8], Vlasov [9], and hybrid [6] simulation studies of ion acceleration from heterogeneous targets. To optimize these beams for applications, one must understand the physics governing their production. In this Letter, we examine the acceleration within a one-dimensional (1D) analytic model.

We consider a substrate of constant density heavy ions with charge Z_I and number density n_I. Initially, the substrate has on it a layer of light ions of negligible thickness and areal charge density Q_i. As in Ref. [10], the electrons comprise two Maxwellians: a hot component (density n_{eh} and temperature T_h), and a cold component (density $n_{ec} \approx$

$n_I Z_I$ and temperature $T_c \ll T_h$). The electron dynamics are rapid, much faster than the ion response, and PIC simulations show that electrons in thin targets recirculate in the electrostatic potential ϕ at the rear target surface [11], so we use a Boltzmann model for the self-consistent electron response. Deep within the foil, E vanishes and the cold and hot electrons attain asymptotic densities $\bar{n}_{eh}$ and $\bar{n}_{ec}$.

The ions have negligible temperature and the substrate and light-ion core charges, $Z_I e$ and $Z_i e$, are held fixed. (Ionization is assumed to occur during the early ramp-up of the sheath E field). During the beam acceleration, the light-ion layer has local charge density much greater than that of the hot electrons. This leads to a Poisson equation of the form

$$\frac{1}{4\pi}\frac{\partial^2 \phi}{\partial x^2} = \bar{n}_{eh}e\exp\left(\frac{e\phi}{T_h}\right) + \bar{n}_{ec}e\exp\left(\frac{e\phi}{T_c}\right) - Q_i\delta(x - x_L) - Z_I n_{I0}e\nu(x), \tag{1}$$

with x_L, the position of the light-ion layer, and $x = 0$, the edge of the substrate. The function $\nu(x) \equiv n_I(x)/n_{I0}$ denotes the relative ion density of the sheath. Initially, $\nu(x) = H(-x)$ (H is the Heaviside function). If we define dimensionless distance $\xi = x/\lambda_{\text{De}} \equiv x\sqrt{4\pi\bar{n}_{eh}e^2/T_h}$, light-ion layer position $\xi_L \equiv x_L/\lambda_{\text{De}}$, potential $\varphi = e\phi/T_h$, light-ion charge $q = Q_i/(\bar{n}_{eh}e\lambda_{\text{De}})$, and substrate charge density $\Theta = Z_I n_I/\bar{n}_{eh}$, Poisson's equation in I-III (regions defined as in Fig. 1) takes dimensionless form

$$\varphi'' = e^{\varphi} - q\delta(\xi - \xi_L) - \Theta\nu(\xi), \tag{2}$$

where primes denote derivatives with respect to ξ. In obtaining this expression, we assume $T_h \gg T_c$, so the cold electron contributions in I-III are formally subdominant and may be neglected; we make this assumption throughout the analysis. For thick (μm and above) foils, $\varphi = \varphi' = 0$ in IV. Hot electron density and temperature, to which the model parameters are scaled, can be obtained in several ways: from simulation, published results (e.g.,
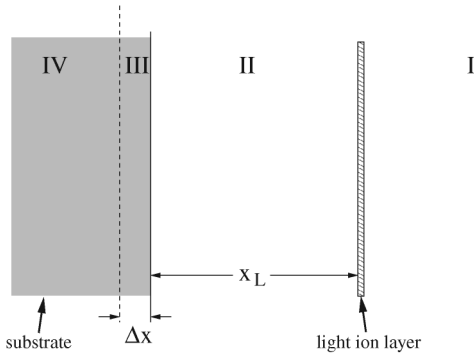
FIG. 1. Sketch of the rear of an expanding laser-driven target with a layer of light atoms initially deposited on a heavy substrate; T_h, T_c, $\bar{n}_{eh}$, and $\bar{n}_{ec}$ are defined in IV as boundary conditions. To the right of the dashed line, cold electrons have been excluded by space charge of the hot electrons. Ions in the light-ion layer and in III are accelerated by the E field in the sheath.

Ref. [12]), or deductions based upon energy/momentum balance (e.g., Ref. [9]). For instance, from energy balance, the hot electron density (in cm^{-3}) at the laser spot is $\bar{n}_{eh} \approx 410 I f/(T_e/m_e c^2)$, with I the laser intensity (W/cm^2), $f \sim 0.5$ the fraction of laser power absorbed by hot electrons, $T_e/m_e c^2 = \sqrt{1 + I\lambda^2/1.4 \times 10^{18}} - 1$, from Ref. [12], and λ the laser wavelength (in μm).

We seek to solve (2) in terms of ξ_L, q, and Θ. In I, (2) is $\varphi'' = e^\varphi$, which is integrated using that $\varphi = -\infty$ and $\varphi' = 0$ as $\xi \to \infty$ to obtain

$$\varphi = -2 \log[e^{-\varphi_{L,I}/2} + (\xi - \xi_L)/\sqrt{2}], \qquad (3)$$

where $\varphi_{L,I} \equiv \lim_{\xi \downarrow \xi_L} \varphi(\xi)$; this result matches that obtained in Ref. [10]. This model is not locally charge neutral; the boundary conditions imply surface charges located far to the right to detach the charge sheath from the substrate.

At the right boundary of II, the matching conditions result in $\varphi_{L,II} = \varphi_{L,I} \equiv \varphi_L$ and $\varphi'_{L,II} = \varphi'_{L,I} + q$. Since $q > 0$ and $\varphi'_{L,I} < 0$, the E field left of the layer is necessarily smaller than that to the right of the layer, as expected. In II,

$$\varphi' = \sqrt{2} p[e^\varphi - (\sqrt{2} q e^{\varphi_L/2} - q^2/2)]^{1/2}, \qquad (4)$$

where $p = \pm 1$. We define

$$a \equiv q[\sqrt{2} e^{\varphi_L/2} - q/2] \qquad (5)$$

proportional to the mean force on the light ions, and require $a > 0$, as required for propagation of a thin layer. When $a < 0$ the ion charge in the layer exceeds that of the electrons in the sheath, so the rightmost light ions expand, leaving the leftmost light ions still attached to the substrate. Upon integration, the solution has two roots, only one of which satisfies boundary conditions φ_0 and φ'_0 and jump conditions across ξ_L. Defining $\gamma \equiv \tan[(\xi_L - \xi)\sqrt{a/2}]$, we get

$$\varphi = \varphi_L + \log(1 + \gamma^2) - 2\log[1 + p\gamma\sqrt{e^{\varphi_L}/a - 1}]. \quad (6)$$

The $p = -1$ solution has φ decreasing over all of II and is appropriate at early time. When the layer propagates far enough that $\varphi_L < 2\log(q/\sqrt{2})$, $p = +1$ and the solution has a local minimum $\varphi = \log a$ at $\xi = \sqrt{2/a}\tan^{-1}\times \sqrt{e^{\varphi_L}/a - 1} \equiv \xi_{\min}$. The $p = -1$ solution positively accelerates all light ions; $p = +1$ has ions at the back of the layer losing momentum in the lab frame.

In III, $\Theta \gg 1$ implies a narrow boundary layer in which the charges of the substrate ions shield the E fields of the sheath. At a distance $\Delta\xi \equiv \Delta x/\lambda_{De}$ within the layer, assuming $T_c \ll T_h$, both φ and φ' vanish. Ignoring hot electron space charge in (2), we find that, initially, $\varphi(\xi) \approx -\frac{1}{2}\Theta(\xi + \Delta\xi)^2$ for $-\Delta\xi \le \xi \le 0$, so at the right of III, $\varphi'_0 \approx -\sqrt{-2\Theta\varphi_0}$. Equations (5) and (6) with the matching condition at the substrate yield a closed set of transcendental equations from which the potential and self-consistent hot electron density in the sheath can be computed. (As in Ref. [10], corrections to this region III solution are needed if the cold electrons are warm enough for the cold electron Debye length to become comparable to the thickness of region III.)

We first consider a substrate of infinite-mass ions. Assuming parameters $q = 0.03$ and $\Theta = 70$, we show in Fig. 2 the form of the dimensionless potential φ as a function of ξ for various ξ_L. The median asymptotic energy $\mathcal{E}$ has been evaluated numerically for $0.003 \le q \le 0.3$ and $10 \le \Theta \le 1000$; this energy is

$$\mathcal{E} = \int_0^\infty d\xi_L \left(\sqrt{2} e^{\varphi_L(\xi_L)/2} - \frac{q}{2} \right), \qquad (7)$$

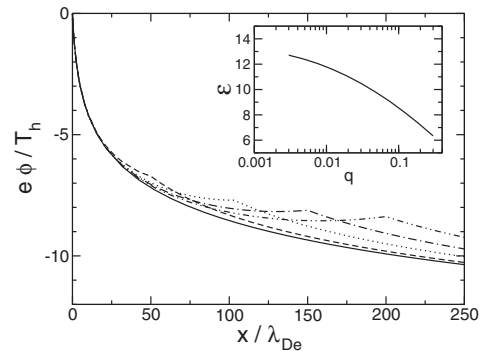and is related to the energy in physical units $E_{\max}$ through

FIG. 2. Potential $\varphi = e\phi/T_h$ as a function of distance ξ (scaled to hot electron Debye length) for propagation of a thin ion layer from an infinite-mass substrate. The ion layer has scaled areal charge density $q = Q_i/(\bar{n}_{eh}e\lambda_{De}) = 0.03$ and the substrate, scaled charge density $\Theta = Z_I n_I/\bar{n}_{eh} = 70$. Shown are potentials with the ion layer at position $x/\lambda_{De} = 0$ (solid line), 50 (dashed line), 100 (dotted line), 150 (dot-dashed line), and 200 (dot-dot-dashed line). The inset shows the scaling of asymptotic light-ion beam energy with dimensionless beam charge density q.

$E_{\max} = Z_i \mathcal{E} T_h$. An empirical fit to the asymptotic energies (to within 2%), satisfies $\mathcal{E} \approx 3.40 - 2.66 \log q - 0.182 (\log q)^2$ (see Fig. 2 inset). The asymptotic energy is insensitive (variation <1%) to Θ in this range.

If the substrate ions have finite mass, the substrate will expand. Since the sheath E field depends on the boundary conditions within the substrate, this expansion affects the energy and quality of the beam. This introduces an additional parameter $R = r_i / r_I$ [$r_i \equiv Z_i/(m_i/m_e)$; similarly for r_I], which Ruhl showed governs detachment of light ions from the substrate [6]: detachment requires $R > 1$. A simple model for the early-time substrate expansion is the following: neglecting ion pressure, an initially constant-density and constant-charge-density substrate with $\Theta \gg 1$ obeys $d^2 \xi / d\tau^2 = -r_I \varphi'$, where $\tau \equiv \omega_{\text{pe}} t$ is scaled time. When $\Theta \gg 1$, hot electron space charge in III can be neglected and one finds $\xi(\tau) = \xi(0) + \tau^2 \Theta r_I [\xi(0) + \delta\xi]/2$, where the initial thickness of region III is $\delta\xi = \sqrt{-2\varphi_0/\Theta}$. Such a layer expands self-similarly: two neighboring ions initially separated by distance ϵ will be separated at time τ by $\epsilon[1 + \tau^2 \Theta r_I/2]$.

This separation is translation invariant within III, so the charge density evolves as $\hat{\Theta}(\tau) = \Theta/[1 + \tau^2 \Theta r_I/2]$ until the space charge of the hot electrons in III can no longer be neglected. Then, the hot electrons Debye shield the sheath E field and the acceleration of the ions is greatly diminished. This occurs at different times for different parts of the expanding substrate. The rightmost ions (which fix the boundary conditions for the sheath) cease to accelerate last, when the expanding ion density becomes comparable to the hot electron density ($\hat{\Theta} \approx 1$); this occurs at time $\tau_f \approx \sqrt{2/r_I}$, corresponding to $t_f \approx 43\omega_{\text{pe}}^{-1} \sqrt{A_I/Z_I}$, with A_I, the atomic mass in amu ($A_I \gtrsim Z_I$, so the expansion is over many ω_{pe}^{-1}, which justifies *a posteriori* the adiabatic electron model). The light-ion layer then propagates with its associated cloud of electrons; exchange of energy between the light ions and the comoving electrons occurs over the remaining propagation distance of the beam.

With this turn-off time, the maximum energy of the heavy ions $E_{I,\max}$ can be computed, using $\xi_{\max} = \Theta \delta\xi \sqrt{2r_I}$, as

$$E_{I,\max} \approx T_h Z_I (\sqrt{2} - q)^2. \tag{8}$$

This relation also predicts ion energy cutoffs in settings for which one has no light-ion layer, in which case $q = 0$.

The equations of motion for the light ions may be integrated numerically using the scaled E field at the center of the layer $-\varphi' = \sqrt{2} \exp(\varphi_L/2) - q/2$. Using the same time cutoff as for the heavy ions, the light ions' final speed is

$$\dot{\xi}_{L,f} = [2.74 + 0.858 \log R + 1.59 (\log R)^2][0.854$$
$$- 0.0312 \log q - 0.00264 (\log q)^2 + 0.0193 \log \Theta] \tag{9}$$

over the range $0.001 \le q \le 0.1$, $10 \le \Theta \le 1000$, and $1.05 \le R \le 16$ (fit to within $\pm 5\%$). This speed is used in $E_0 = m_i Z_I T_h \dot{\xi}_{L,f}^2 / 4m_I$ to estimate the mean energy of the light ions. The product $Z_I \dot{\xi}_{L,f}^2$ increases with increasing Z_I, so for fixed substrate material, the higher the substrate charge, the higher the asymptotic energy: the substrate comoves longer with the light ions, so the latter accelerates longer before detaching from the substrate. This charge-to-mass ratio dependence is qualitatively consistent with the double-layer foil target experiments of Badziak *et al.* [13], where higher peak proton energy resulted from a poly-styrene layer at the rear of an Au foil compared with heavier substrates.

We estimate, if in a rough way, the energy spread of the beam: in pure 1D expansion, the initial charge density of light ions is much larger than that of hot electrons, so the dominant energy spread is from space-charge expansion of the light ions. We assume a uniform slab of light ions, so in the frame of the center of mass (c.m.) of the slab, the distance $\delta x_i(t)$ an ion moves obeys $d^2 \delta x_i / dt^2 \approx \omega_{\text{pi}}^2 \delta x_i(0)$; expansion continues until $Z_i n_i \approx \bar{n}_{eh} e^{\varphi_L}$, when the electrons shield the layer. (Further quasineutral evolution is slower and leads to less energy accrual [14]). A layer with finite transverse extent $L \gg \delta x_i(0)$ has an additional upper bound on energy spread ΔE as a result of the 3D divergence of the E field. The layer expands as a 1D layer until $\delta x_i(t) \sim L$. Then, the layer accelerates more slowly, reaching speed comparable to the asymptotic speed of a spherical expansion in the moving frame. (The asymptotic speed of an expanding, initially uniform-density sphere of light ions with radius L and total charge equal to that of the light-ion layer is within an $\mathcal{O}(1)$ factor of the maximum speed of light ions in the c.m. frame when the layer expands to thickness L). This model predicts $(\Delta E/E_0)_{1D} \approx \sqrt{q^2 e^{-\varphi_L} Z_i T_h / E_0}$ and $(\Delta E/E_0)_{3D} \approx \min\{(\Delta E/E_0)_{1D}, \sqrt{Z_i q L T_h / 3 \lambda_{\text{De}} E_0}\}$ in 1D and 3D geometry, respectively. In 3D, high transverse localization of the beam, e.g., beams forming from "microdots" [8], can enhance beam quality over what one gets from an infinite 1D layer of the same thickness.

We have compared the theory with results from 1D simulations using VPIC [15]. The simulation used a 100 μm domain with a 10 μm thick Pd foil 4 μm from the left boundary. A thin ($\sim$0.005 μm) layer of protons was deposited at the rear surface and the Pd density had a ramp of 1 μm on the front region. The substrate, of peak density $n_{\text{Pd}} = 2.23 \times 10^{22}$ cm^{-3}, and the protons ($n_p = 2.23 \times 10^{22}$ cm^{-3}, deposited with a linear density ramp over the layer) were singly ionized. The initial electron temperature was 5 keV. The pulse was 238 fs with peak intensity $I = 10^{20}$ W/cm^2. In the target, 1000 simulation particles/cell of each species were used. As seen in the top panel in Fig. 3, E_x from theory (dotted curves) is in agreement with the simulations (solid curves). This agreement is remarkable considering that the parameters
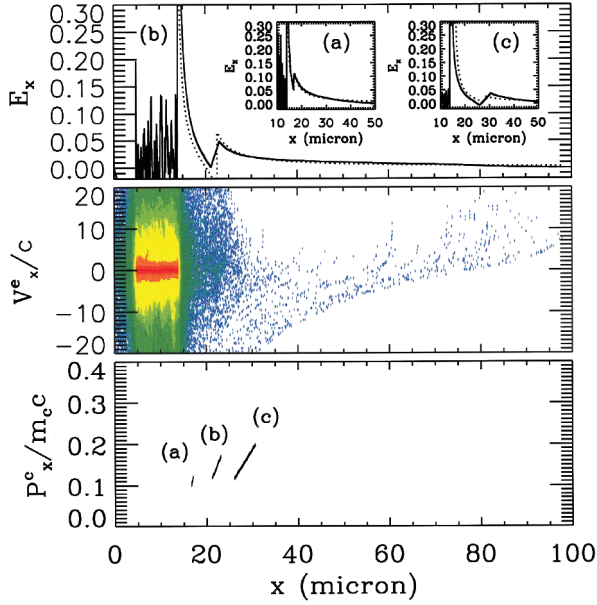
FIG. 3 (color). Comparison of 1D VPIC simulation of proton ion acceleration from a palladium substrate. The laser is incident from the left. The top panel is E_x at time (b) $t = 2937\omega_{pe}^{-1}$ from the laser turn-on: the solid curve is the simulation data, the dashed curve, the analytic solution. The insets show E_x at earlier (a) $t = 1774\omega_{pe}^{-1}$ and later (c) $t = 4100\omega_{pe}^{-1}$ time. The second and third panels are electron (log scale) and proton phase spaces; the former is at time (b) and the latter, at times (a),(b), and (c), as indicated.

used in the theory were obtained from empirical scaling laws—Wilks scaling [12] for T_e ($7.51m_ec^2$), absorption fraction $f = 0.5$, and electron density as above ($n_e = 2.71 \times 10^{21}$ cm^{-3})—and that the light-ion layer is rather thick and therefore only weakly satisfies the scale-separation assumptions of the model. (This would not have been so had we propagated the light ions as Lagrangian tracers in the sheath, as in earlier studies [8,16]). Electron and proton phase spaces are shown (lower panels, logarithmic density scales). We also compare asymptotic energies of the protons and palladium ions, using parameters $q = 0.0735$, $\Theta = 8.23$, and $R = 106.4$. At $t = 6427\omega_{pe}^{-1} \sim$ 1 ps (after the laser has turned off) the predicted proton energy is 14.2 MeV from (9) (simulation: 13.5 MeV); predicted Pd peak energy is 6.9 MeV (simulation: 4.0 MeV). Beam quality is $\Delta E/E_0 = 82\%$ (simulation: 73%).

We further validate the theory by comparison to experimental data. Hegelich *et al.* [6] report that hybrid modeling of their experiment leads to inferred temperature $T_h = 2.5$ MeV and hot electron density $n_h = 10^{21}$ cm^{-3}. The most energetic substrate ions had ionization state Pd^{22+}, for which $\Theta = 1500$. The initial areal carbon density, inferred from ion counts on the radiochromic film at the back of a Thomson parabola spectrometer, gave $q \approx 0.03$. The ratio of c.m. ratios for C^{5+} and Pd^{22+} is 2.02. With these values in (8) and (9), we obtain 2.15 MeV/nucleon

for C^{5+} and 1.01 MeV/nucleon (max energy) for Pd^{22+}, values consistent with the measured energies for C^{5+} (3.0 MeV/nucleon mean energy) and Pd^{22+} (2.0 MeV/nucleon maximum). The predicted energy spread (assuming $\sim 15\ \mu$m transverse thickness) is $\Delta E/E_0 = 0.26$, compared with 0.16 in the experiments.

*Guest scientist.
Present address: D. E. Shaw Research LLC, 120 W. 45th St., NY, NY 10036, USA.
[1] R. A. Snavely, M. H. Key, S. P. Hatchett, T. E. Cowan, M. Roth, T. W. Phillips, M. A. Stoyer, E. A. Henry, T. C. Sangster, and M. S. Singh *et al.*, Phys. Rev. Lett. **85**, 2945 (2000).
[2] B. M. Hegelich, S. Karsch, G. Pretzler, D. Habs, K. Witte, W. Geunther, M. Allen, A. Blazevic, J. Fuchs, and J. C. Gauthier *et al.*, Phys. Rev. Lett. **89**, 085002 (2002).
[3] B. M. Hegelich, B. Albright, P. Audebert, A. Blazevic, E. Brambrink, J. Cobble, T. Cowan, J. Fuchs, J. C. Gauthier, and C. Gautier *et al.*, Phys. Plasmas **12**, 056314 (2005).
[4] A. Maksimchuk, S. Gu, K. Flippo, D. Umstadter, and V. Y. Bychenkov, Phys. Rev. Lett. **84**, 4108 (2000).
[5] M. Temporal, J. J. Honrubia, and S. Atzeni, Phys. Plasmas **9**, 3098 (2002).
[6] B. M. Hegelich, B. J. Albright, J. Cobble, K. Flippo, S. Letzring, M. Paffett, H. Ruhl, J. Schreiber, R. K. Shulze, and J. C. Fernández, Nature (London) **439**, 441 (2006).
[7] H. Schwoerer, S. Pfotenhauer, O. Jäckel, K. U. Amthor, B. Liesfield, W. Ziegier, R. Sauerbrey, K. W. D. Ledingham, and T. Esirkepov, Nature (London) **439**, 445 (2006).
[8] T. Z. Esirkepov, S. V. Bulanov, K. Nishihara, T. Tajima, F. Pegoraro, V. S. Khoroshkov, K. Mima, H. Daido, Y. Kato, and Y. Kitagawa *et al.*, Phys. Rev. Lett. **89**, 175003 (2002).
[9] A. P. L. Robinson, A. R. Bell, and R. J. Kingham, Phys. Rev. Lett. **96**, 035005 (2006).
[10] M. Passoni, V. T. Tikhonchuk, M. Lontano, and V. Y. Vychenkov, Phys. Rev. E **69**, 026411 (2004).
[11] Y. Sentoku, T. E. Cowan, A. Kemp, and H. Ruhl, Phys. Plasmas **10**, 2009 (2003).
[12] S. C. Wilks, W. L. Kruer, M. Tabak, and A. B. Langdon, Phys. Rev. Lett. **69**, 1383 (1992).
[13] J. Badziak, E. Woryna, P. Parys, K. Y. Platonov, S. Jabloński, L. Ryé, A. B. Vankov, and J. Wolowski, Phys. Rev. Lett. **87**, 215001 (2001).
[14] P. Mora, Phys. Rev. Lett. **90**, 185002 (2003).
[15] The explicit, 3D, relativistic, fully electromagnetic, particle-in-cell code VPIC was designed by Kevin Bowers in the LANL X-1 group, where it is currently maintained.
[16] E. Fourkal, I. Velchev, and C.-M. Ma, Phys. Rev. E **71**, 036412 (2005).